

Open-Set Text Recognition via Character-Context Decoupling

Chang Liu¹ Chun Yang^{1,*} Xu-Cheng Yin^{1,2,*}

¹ School of Computer and Communication Engineering, University of Science and Technology Beijing

² Institute of Artificial Intelligence, University of Science and Technology Beijing, China

lasercat@gmx.us, {chunyang, xuchengyin}@ustb.edu.cn

Abstract

The open-set text recognition task is an emerging challenge that requires an extra capability to cognize novel characters during evaluation. We argue that a major cause of the limited performance for current methods is the confounding effect of contextual information over the visual information of individual characters. Under open-set scenarios, the intractable bias in contextual information can be passed down to visual information, consequently impairing the classification performance. In this paper, a Character-Context Decoupling framework is proposed to alleviate this problem by separating contextual information and character-visual information. Contextual information can be decomposed into temporal information and linguistic information. Here, temporal information that models character order and word length is isolated with a detached temporal attention module. Linguistic information that models n -gram and other linguistic statistics is separated with a decoupled context anchor mechanism. A variety of quantitative and qualitative experiments show that our method achieves promising performance on open-set, zero-shot, and close-set text recognition datasets.

1. Introduction

Text recognition is a well-studied task and has been widely applied in various applications [7]. Most existing text recognition methods assume characters in the testing set are covered by the training set. Moreover, consistency of contextual information between the training set and the testing set is also assumed. These methods are not adaptable to recognize unseen characters without retraining the model. However, as the language evolves, novel ligatures (e.g., rare characters, emoticons, and foreign characters) can be frequently used in a region during a certain period. For example, foreign characters can be seen frequently in scene text images as a result of globalization. Hence, it is

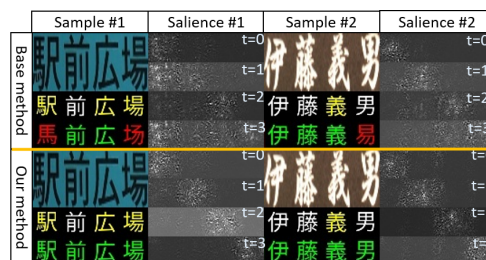


Figure 1. Illustration of the “saliency region” [37] of each time-step, showing where the models look at. Base model (top) tends to seek the help from the context, while our framework (bottom) focuses more on local character features.

unfeasible if the model needs to be retrained whenever a “new character” emerges. This task is defined as the open-set text recognition task [23], as a specific field of open-set recognition [33] and a typical case of robust pattern recognition [54]. Currently, a few visual-matching-based text recognition methods are capable to recognize novel characters in text lines [16, 23, 52].

However, these open-set text recognition methods tend to be affected by contextual information captured from the training set. This phenomenon can be seen in the saliency map (Fig. 1) ¹, and is also observed in [41]. In such cases, feature representation for each character is always mixed with linguistic information. This could benefit close-set scenarios where the contextual information bias between training and evaluation is negligible, as some characters (e.g. ‘0’ and ‘O’) are hard to separate only by character visual information (glyph shapes). However, under open-set scenarios, contextual information could be severely biased from the training set. Consequentially, existing models may mistakenly “correct” a character into a wrong one that fits “better” in the context according to the training set [41].

To alleviate the impact of contextual information over open-set text recognition, we propose a character-context decoupling framework allowing explicit separation of character visual information and contextual information. Con-

*Corresponding authors.

¹<https://github.com/MisaOgura/flashtorch>

textual information is further decomposed into temporal information and linguistic information. In general, temporal information models the number and order of characters in a word, while linguistic information models n-gram and other linguistic statistics. Accordingly, a Detached Temporal Attention module (DTA) is introduced to model temporal information and isolate it from visual features. Also, a Decoupled Context Anchor mechanism (DCA) is proposed to “explain away [47]” the linguistic information from character visual information. In summary, our framework reduces the confounding effect of training-set contextual information on visual features, making it less vulnerable to the intractable contextual information bias under open-set scenarios.

The main contributions of this paper are summarized as follows:

- (1) Proposing a Character-Context Decoupling Framework that improves word-level open-set text recognition by reducing the effect of contextual information on the visual representation of novel characters in word-level samples.
- (2) Proposing a Detached Temporal Attention module that reduces the impact of temporal information over the visual feature extractor.
- (3) Proposing a Decoupled Context Anchor mechanism that enables the separation of linguistic information from the visual feature extractor.

2. Related Work

Open-set text recognition, as a specific field of open-set recognition [13, 33], is a task that requires the model to recognize testing-set words that may contain novel characters unseen in the training set [23]. A few methods [23, 52] have been proposed to address this task. Wan *et al.* [52] proposed to match the visual features of the word image with the glyph image, and to sample the matching results with a class aggregator. Their method does not scale well on large-scale character sets due to the size growth of the glyph images and the similarity maps. On the other hand, OSOCR [23] generates class centers from individual glyphs with a ProtoCNN and matches the class centers with serialized visual features of the word image. The character-based prototype generating design allows reducing the training cost by mini-batching the label set, thus can be applied to larger label-sets. However, these methods [23, 52] do not provide effective approaches to separate contextual information, limiting the performance of open-set word-level recognition. Impacts of contextual information are also studied in [41], which suggests that RNN-free methods are also prone to contextual information bias. Hence, we propose a framework that decouples and isolates contextual information from character visual information to improve open-set visual-matching accuracy.

The conventional close-set text recognition tasks can be considered as a special case where the testing set has zero

novel characters. In most conventional text recognition methods [3, 20, 34, 44, 48], class centers are mostly modeled as weights in linear classifiers, while visual information and contextual information are modeled together without explicit separation. Recently, more methods opt to adopt dedicated post-processing fashioned modules [11, 49] to model contextual information.

The zero-shot character recognition task is another special case of open-set text recognition. Many methods [4, 6, 16, 43, 45] propose to encode each character with a unique structural representation (e.g., radical or stroke sequences) for prediction. Recently, a few methods demonstrate capabilities for Korean character recognition [6] and whole word recognition [16]. Despite performing reasonably well with large label sets, these methods require language-specific structural representations of characters, thus limit them to corresponding languages. In contrast, structure-free methods like [1, 23] only require a template from a font (or a printed sample) for each character. This approach benefits scenarios where little prior knowledge of character composition can be given, for example, ancient writings of the Oracle characters. Our method follows the structure-free scheme and further achieves reliable word recognition capability by introducing character-context decoupling.

3. Proposed Method

In this work, we propose a character-context decoupling framework (shown in Fig. 2) to reduce the impact of contextual information bias under open-set scenarios, by separating and isolating character visual information and contextual information with the Detached Temporal Attention module and the Decoupled Context Anchor mechanism. The framework and its optimization are first formulated in Section 3.1. Then, a detailed explanation of the less intuitive Decoupled Context Anchor mechanism is presented in Section 3.2. Finally, the Open-set Character-Context Decoupling network (OpenCCD) is given as an example implementation of our framework in Section 3.3.

3.1. Character-Context Decoupling Framework

The framework takes a sample (word-level image) img and a character set E as input, and outputs the predicted word $\hat{y} : (\hat{y}_{[0]}, \dots, \hat{y}_{[t]})$ with the maximum probability given the sample and character set,

$$\hat{y} = \arg \max_{\mathbf{y}} P(\mathbf{y} | \mathbf{x}, E; \theta), \quad (1)$$

where \mathbf{x} is the visual feature representation of all characters in the sample. We omit the E and θ in the following part for writing convenience. In our framework, we expand $P(\mathbf{y} | \mathbf{x})$ with a predicted length l , using the law of total probability,

$$P(\mathbf{y} | \mathbf{x}) = \sum_{l=1}^{maxL} P(l | \mathbf{x}) P(\mathbf{y} | \mathbf{x}, l), \quad (2)$$

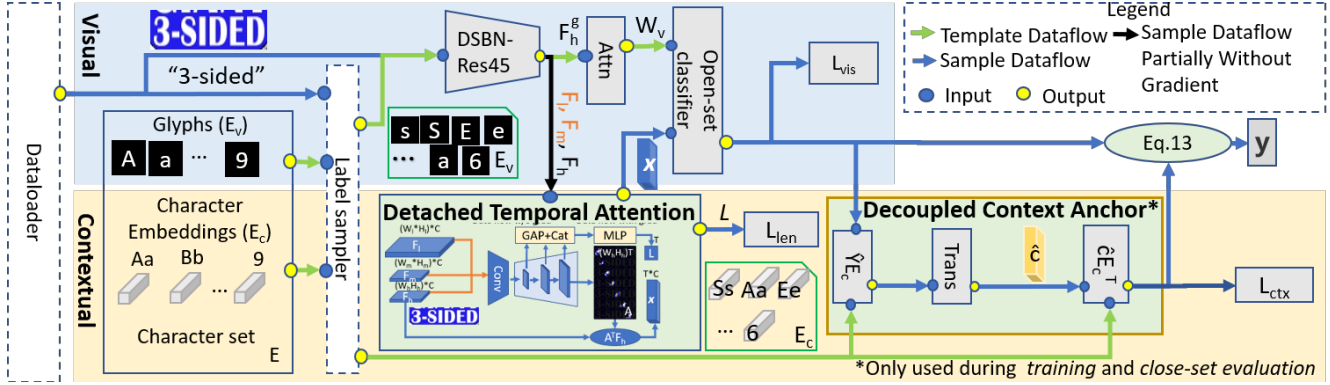


Figure 2. Our implementation of the proposed Character-Context Decoupling Framework. In the framework, visual representation of the sample and character templates are first extracted with the DSNB-Res45 Network [5], then the Detached Temporal Attention module predicts the word length and samples visual features $x_{[t]}$ for each timestamp. The visual prediction is achieved by matching prototypes (attention-reduced template features) with the Open-set classifier. Finally, the visual prediction is adjusted with the Decoupled Context Anchor module, and no adjustment is conducted when there is intractable linguistic information under open-set scenarios.

where $maxL$ is the maximum length of a word. Different from most existing text recognition frameworks using end-of-speech [35, 44], segmentation [21, 40], or blanks [9, 34] to handle lengths, our framework explicitly predicts the length. $P(\mathbf{y}|\mathbf{x}, l)$ can be further decomposed to contextual prediction and visual prediction via the proposed Decoupled Context Anchor mechanism (detailed in Section 3.2),

$$P(\mathbf{y}|\mathbf{x}, l) = \prod_{t=1}^l P(y_{[t]}|x_{[t]}) \prod_{t=1}^l \int^{c \in C_{[t]}} P(y_{[t]}|c)P(c|\mathbf{x}, l). \quad (3)$$

Here, c is the common ‘‘context’’ (linguistic information) of characters, \mathbf{x} models the visual information of all characters in the input image, and $x_{[t]}$ corresponds to the character visual information of the t^{th} character. Hence, the optimization goal would be maximizing the log-likelihood $logP(\mathbf{y}^*|\mathbf{x})$ of the ground truth label sequence \mathbf{y}^* ,

$$\begin{aligned} & logP(\mathbf{y}^*|\mathbf{x}) \\ &= log\left(\sum_{l=1}^{maxL} P(l|\mathbf{x})P(\mathbf{y}^*|\mathbf{x}, l)\right) \\ &\stackrel{(a)}{=} logP(l^*|\mathbf{x}) + logP(\mathbf{y}^*|\mathbf{x}, l^*) \\ &= logP(l^*|\mathbf{x}) + \sum_{t=1}^{l^*} (logP(y_{[t]}^*|x_{[t]})) \\ &\quad + \sum_{t=1}^{l^*} log\left(\int^{c \in C_{[t]}} P(y_{[t]}^*|c)P(c|\mathbf{x}, l^*)\right) \\ &:= -(L_{len} + L_{vis} + L_{ctx}), \end{aligned} \quad (4)$$

where L_{len} , L_{vis} , and L_{ctx} are the corresponding cross-entropy losses of the three loglikelihood terms. Step (a)

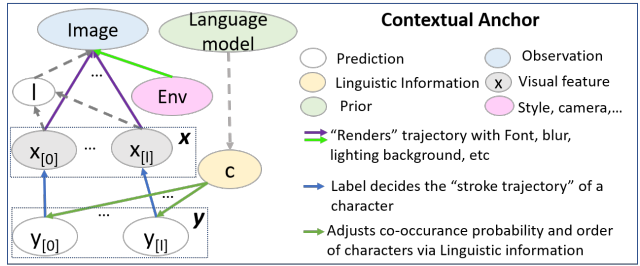


Figure 3. Causal graph of our Decoupled Context Anchor mechanism.

holds because the correct label can only be predicted when the length is correctly predicted.

3.2. Decoupled Context Anchor Mechanism

In this work, we propose a Decoupled Context Anchor mechanism to model and separate the effect of linguistic information c over character $y_{[t]}$ at each timestamp t .

Assumption 1 (A1) We assume the linguistic information functions as a common-cause of the input visual information and the prediction outputs at all timestamps (See Fig. 3). We model the sample image as a ‘‘rendered’’ result of the label \mathbf{y} . Also, we assume the label (words) is generated according to linguistic information c , making the label \mathbf{y} a causal result of c . Hence, linguistic context c and the character-level visual information $x_{[t]}$ are the only two direct factors affecting the probability of $y_{[t]}$ at timestamp t ,

$$P(y_{[t]}|x_{[t]}, \mathbf{x}, y_{[t-1]} \dots y_{[0]}, l, c) = P(y_{[t]}|x_{[t]}, c), \quad (5)$$

Assumption 2 (A2) The shape (character visual information) of a character and its context (linguistic information)

are independent given the character $y_{[t]}$, i.e.,

$$\begin{aligned} P(x_{[t]}|y_{[t]}, c) &= P(x_{[t]}|y_{[t]}) \\ \iff P(x_{[t]}, c|y_{[t]}) &= P(x_{[t]}|y_{[t]})P(c|y_{[t]}). \end{aligned} \quad (6)$$

This assumption implies that the linguistic information does not affect the “style” (font face, color, background, etc.) of the word, which generally holds in most synthetic datasets where styles and contents are randomly matched.

Theorem 1: The Anchor Property of Context

Given assumption A1, the probability of a predicted word \mathbf{y} given image \mathbf{x} and its length l , $P(\mathbf{y}|\mathbf{x}, l)$, can be written as the product of the “anchored predictions” of all time-steps, i.e.,

$$P(\mathbf{y}|\mathbf{x}, l) = \prod_{t=1}^l \int_{c \in C_{[t]}} P(y_{[t]}|x_{[t]}, c)P(c|\mathbf{x}, l), \quad (7)$$

and the proof is detailed in Appendix A. Here, the integral term can be interpreted as an ensemble of “anchored prediction” $P(y_{[t]}|x_{[t]}, c)$ over all possible contexts c , which is similar to the hidden anchor mechanism [15]. Hence, we call this theorem the anchor property of context.

Theorem 2: The Separable Property of Linguistic Information and Character Visual Information

Given Assumption A2, the effect of character visual information over the label $P(y_{[t]}|x_{[t]})$ and the effect of linguistic information $P(y_{[t]}|c)$ is separable from contextual prediction $P(y_{[t]}|x_{[t]}, c)$,

$$P(y_{[t]}|x_{[t]}, c) \propto \frac{P(y_{[t]}|x_{[t]})P(y_{[t]}|c)}{P(y_{[t]})}. \quad (8)$$

Here, $P(y_{[t]}|x_{[t]})$ represents the predicted probability of $y_{[t]}$ with regard to character visual information $x_{[t]}$, $P(y_{[t]}|c)$ models the effect caused by linguistic information, and $P(y_{[t]})$ models the character frequency on the training set. The proof of this theorem is given in Appendix B. This theorem suggests that the effect of character visual information and linguistic information over the prediction can be **explicitly** separated under specific conditions.

Intuitively, $P(y_{[t]}|c)$ “explains away” [47] the linguistic information from the visual-based prediction $P(y_{[t]}|x_{[t]})$. This behavior happens in the backpropagation pass of our framework during training, where the gradients of L_{ctx} and L_{vis} are accumulated to update the feature extractor. This is the reason that L_{ctx} needs to be backpropagated, and also makes L_{ctx} a regularization term, in terms of enforcing certain properties of the network via backpropagation. This property differentiates it from the “look-twice” mechanisms [11, 49] that cut gradients.

Theorem 3: Decoupled Context Anchor Mechanism

Combining Theorem 1 and Theorem 2, we have the Decoupled Context Anchor mechanism,

$$\begin{aligned} P(\mathbf{y}|\mathbf{x}, l) &= \prod_{t=1}^l P(y_{[t]}|x_{[t]}) \prod_{t=1}^l \int_{c \in C_{[t]}} P(y_{[t]}|c)P(c|\mathbf{x}, l). \end{aligned} \quad (9)$$

Proof of this theorem can be found in Appendix C. The mechanism further allows explicit separation of linguistic information and character visual information on the **word** level, which provides a way to model and separate linguistic information learned on the training set, resulting in a feature extractor focusing more on character visual information and less affected by the training set linguistic information. Considering the anchor property revealed in Theorem 1 and the decoupling nature of Theorem 2, we call this mechanism the Decoupled Context Anchor mechanism.

3.3. OpenCCD Network

In this section, the Open-set Character-Context Decoupling network (OpenCCD, Fig. 2) is given as an example implementation of our proposed framework. Here, character set $E : (E_v, E_c)$ consists of glyphs from the Noto font E_v and semantic embeddings of the characters E_c . The network first extracts visual features of the word images img and the glyphs E_v with the 45-layer ResNet built with DSBN [5] layers (Res45-DSBN). It shares the convolutional layers between the glyphs and word images, while keeping task-specific batch statistics. Three levels of word features (F_l, F_m, F_h) and the latest feature map F_h^g of glyphs are used. The prototypes (class centers) W_v are generated by applying geometric attention to F_h^g . During training, we mini-batch E_v at each iteration to achieve a reasonable training speed. During the evaluation, the visual prototypes W_v for the whole dataset are cached beforehand, hence prototype generation yields little extra costs.

Next, the Detached Temporal Attention (DTA) module is used to predict the length of the word $P(l|\mathbf{x})$, and the max probable length is denoted as \hat{l} . Then the DTA module samples ordered character-level visual features $\mathbf{x} : (x_{[0]}, \dots, x_{[\hat{l}]})$ from the feature map F_h .

The visual-based prediction $P(y_{[t]}|x_{[t]})$ is then produced by the open-set classifier. For close-set scenarios, the linguistic information oriented prediction $P(y_{[t]}|c)$ is produced via the Decoupled Context Anchor (DCA) module. For open-set scenarios where linguistic information is intractable, $P(y_{[t]}|c)$ is treated as a uniform distribution, which is equivalent to only using the visual prediction.

Detached Temporal Attention In OpenCCD, the detached temporal attention module (Fig. 4) is proposed to

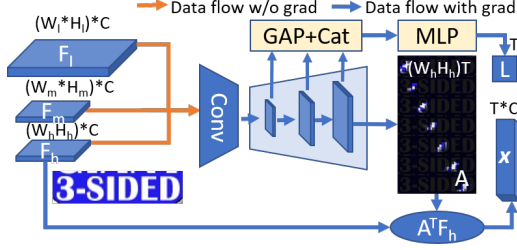


Figure 4. The proposed detached temporal attention module. We isolate sequence modeling within the Temporal Attention module, and zero the gradient of convolution features, w.r.t., the temporal attention map. Here, GAP indicates a global-average pooling.

predict the sequence length $P(l|\mathbf{x})$. It also sort and sample character in feature map F_h via the attention map A . The module utilizes an FPN to model global temporal information from the input feature maps, and decodes them into A and $P(l|\mathbf{x})$. Since temporal information is not related to individual character shapes (character visual information), the module novelly isolates it from input visual feature maps by cutting the gradients w.r.t. $P(l|\mathbf{x})$ and A . The module then segments input visual feature map F_h into visual features \mathbf{x} for individual characters according to attention map A and the most probable length \hat{l} , allowing only character visual information backpropagating to F_h via \mathbf{x} . In OpenCCD, $P(y_{[t]}|x_{[t]})$ is produced by comparing the prototypes with character-level features $x_{[t]}$,

$$P(y_{[t]}|x_{[t]}) \propto \begin{cases} \alpha|x_{[t]}| & y_{[t]} \text{ is [UNK]} \\ |x_{[t]}| \text{Sim}(x_{[t]}, y_{[t]}) & \text{otherwise,} \end{cases} \quad (10)$$

where $|x_{[t]}|$ is the L2-Norm of $x_{[t]}$, “[UNK]” indicates unknown characters, and α is a trainable similarity threshold for rejection. $\text{Sim}(x_{[t]}, y_{[t]})$ is defined as

$$\text{Sim}(x_{[t]}, y_{[t]}) := \max_{w_v \in \psi(y_{[t]})} (\cos(w_v, x_{[t]})), \quad (11)$$

where ψ returns all prototypes $\psi(y_{[t]}) \subset W_v$ associated with label $y_{[t]}$, and each individual prototype w_v corresponds to a “case” of character $y_{[t]}$.

Decoupled Context Anchor Instead of implementing a Variational Auto Encoder [19] to estimate the distribution of linguistic information and estimate the integral with Monte-Carlo, we approximate the integral with predicted context \hat{c} , which is similar to the conventional anchor mechanisms using only the anchor with maximum prediction likelihood [30, 31],

$$\int^{c \in C_{[t]}} P(y_{[t]}|c)P(c|\mathbf{x}, l) \approx P(y_{[t]}|\hat{c}). \quad (12)$$

Combined with Eq. 21, the probability of a predicted character at timestamp t can be approximated as,

$$P(y_{[t]}|\mathbf{x}) \approx P(y_{[t]}|x_{[t]})P(y_{[t]}|\hat{c}). \quad (13)$$

As linguistic information is mostly related to labels, we estimate the linguistic information \hat{c} from the predicted label instead of the feature map. More specifically, the module reuses the estimated character probability distribution $Y \in (0, 1)^{l \times M} : (P(\mathbf{Y}_{[0]}|x_{[0]}), \dots, P(\mathbf{Y}_{[l]}|x_{[l]}))$ with regard to character visual information at each timestamp t , and $P(\mathbf{Y}_{[t]}|x_{[t]}) : (P(y_{[t]}^0|x_{[t]}), \dots, P(y_{[t]}^M|x_{[t]}))$ is the probability distribution of all characters at timestamp t . Then \hat{c} is estimated with a 4-layer transformer encoder [39] applied on the expectation of character embeddings,

$$\hat{c} = \text{Trans}(Y E_c), \quad (14)$$

where $E_c \in R^{M \times C}$ is the semantic embedding of seen characters in the training set, hence $Y E_c$ interprets as expectation. Trans indicates the 4-layer transformer encoder. Finally, $P(\mathbf{Y}_{[t]}|\hat{c})$ is estimated by comparing character embedding E_c to \hat{c} ,

$$P(\mathbf{Y}_{[t]}|\hat{c}) = \sigma(\hat{c} E_c^T)_{[t]}, \quad (15)$$

where σ is the softmax function.

Optimization With Eq. 12 reducing the integral down to a standard classification problem, L_{ctx} in Eq. 4 can be implemented as a cross-entropy loss like L_{len} and L_{vis} . Hence, OpenCCD can be optimized with the three equally-weighted cross-entropy losses.

4. Experiments

The work is based on the OSOCR [23], our code² and datasets³ are released. We conduct experiments on benchmarks for all three scenarios: open-set word-level recognition, zero-shot character recognition, and the conventional close-set word-level recognition benchmarks. Moreover, the ablative studies for open-set word-level recognition are also performed. We use the AdaDelta optimizer, the learning rate is set to 10^{-2} , and decreases by every 200k iterations. For word recognition tasks, we provide a “large” network for an alternative speed-performance trade-off profile closer to SOTA methods, where the large network has more latent channels in the ResNet45-DSBN backbone.

4.1. Open-Set Text Recognition

We use a collection of Chinese text recognition datasets as the training set and the Japanese subset of MLT as

²<https://github.com/lancercat/VSDf>

³<https://www.kaggle.com/vsdf2898kaggle/osocrtraining>

Table 1. Detailed performance analysis on the open-set text recognition dataset. Performance data listed in Character Accuracy (top) / Line Accuracy (bottom) manner.

Method	OSOCR [23]	OSOCR Large [23]	Ours	Ours Large
Kana	-	18.75	43.55	47.35
		0.10	7.52	11.17
Shared Kanji	-	79.86	76.48	76.53
		73.81	74.15	74.66
Unique Kanji	-	71.74	77.50	82.20
		34.08	48.81	58.33
All Kanji	-	75.33	77.06	79.74
		51.64	59.81	65.42
Overall	47.89	49.10	62.16	65.34
	29.08	30.08	36.57	41.31

the testing set following OSOCR [23], and all models are trained for 200k iterations. Quantitative performances are shown in Table 1 along with SOTA methods, and qualitative samples can be found in Fig 5. The results show overall significant performance improvement over OSOCR [23]. Details suggest the performance gain comes from recognizing unseen characters. The model shows some extent of robustness over novel characters (text with yellow color in Fig. 5) like unique Kanjis and Kanas.

Results indicate that characters having close shapes are the most significant source of mistakes. The reason for this phenomenon could be pushing all negative classes alike with hard labels (in contrast to soft-label), which is also mentioned in fine-grain classification [53]. Blur, text art can be another major cause for the failure cases, which is expected as linguistic information is intractable under open-set scenarios, consequently cannot be used to recover the visually indistinguishable characters.

4.2. Ablative Study

We conduct ablative studies on the open-set text recognition challenge to validate the effect of decoupling character visual information and contextual information. In this section, we train all ablative models on the same server to minimize the confounding factors, the results (Fig. 6) show that isolating temporal information with the Detached Temporal Attention module can improve the open-set recognition performance. Also, further separating linguistic information with the Decoupled Context Anchor mechanism is proved to yield more improvement.

Intuitively, test-set accuracy curves show that both proposed approaches introduce a steady performance improvement on most iterations. The instability of the curves is caused by the Line Accuracy metric where one wrong char-



Figure 5. Sample results from the open-set text recognition task. The figure shows qualitative performance under the ‘‘Kana’’, ‘‘Unique Kanji’’ and ‘‘Shared Kanji (close-set)’’ scenarios. The results for each group are represented with two rows, where the top row shows the success cases and the bottom row shows failure cases. Text in white indicates seen characters, yellow indicates novel characters, red indicates recognition error, green indicates correct results, and purple block indicates rejected results.

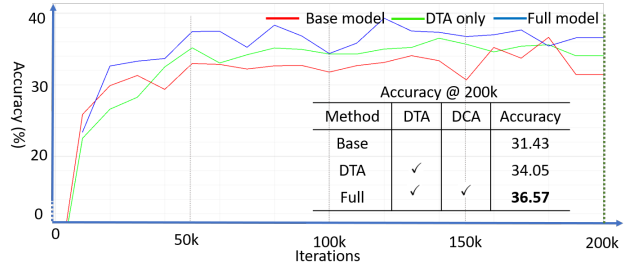


Figure 6. Ablative study on modules proposed. X-axis indicates total iteration and Y-axis indicates test-set accuracy. Steady-performance gain can be achieved after applying each module (Red: base model; green: detaching character visual information; blue: detaching both).

acter can compromise the whole line. We further perform paired *t*-tests to quantitatively validate the robustness of the performance improvements. Separating temporal information with the DTA module shows a 2.00 *t*-value and 0.06 *p*-value, while using DCA to separate linguistic information gives a 5.87 *t*-value and 1.54×10^{-5} *p*-value. The *p*-values suggest we can reject the ‘‘two-sided’’(no improvement) null hypothesis for both approaches. Hence, there is strong evidence that both DTA and DCA can robustly improve the open-set recognition performance.

Qualitatively, we show the result comparison between our model and the base model in Fig. 7. Our framework demonstrates decent robustness improvement against the linguist information bias compared to the base model by separating linguistic information and character visual infor-

Table 2. Zero-shot character recognition accuracy on HWDB and CTW datasets. * indicates “online trajectory” data required.

Method	Venue	Accuracy (%)							
		HWDB				CTW			
		# characters in training set				# characters in training set			
		500	1000	1500	2000	500	1000	1500	2000
CM* [1]	ICDAR'19	44.68	71.01	80.49	86.73	-	-	-	-
DenseRan [46]	ICFHR'18	1.70	8.44	14.71	63.8	0.12	1.50	4.95	10.08
FewRan [43]	PRL'19	33.6	41.5	63.8	70.6	2.36	10.49	16.59	22.03
HCCR [4]	PR'20	33.71	53.91	66.27	73.42	23.53	38.47	44.17	49.79
OSOCR [23]	-	46.67	72.19	79.82	84.31	27.94	48.23	58.56	63.77
Ours	-	90.93	94.10	94.58	95.55	58.22	68.56	74.45	77.18

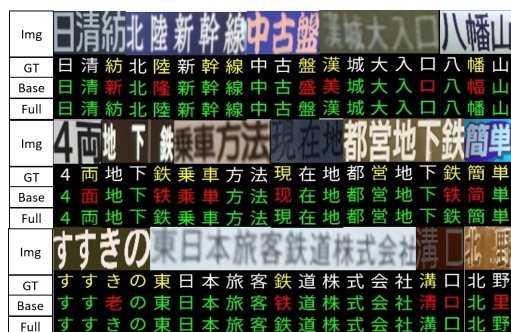


Figure 7. Comparison between our method and the base method. Green indicates correct predictions, red indicates wrong predictions. Yellow indicates novel characters and white indicates seen characters.

mation.

4.3. Conventional Benchmarks

Due to the lack of open-set text recognition benchmarks, we adopt two well-studied special cases to give referenced comparisons on generalization capability and word recognition capability. Here, we stick to the most applied protocols in each corresponding community to train, evaluate, and measure the performances.

Zero-Shot Character Recognition Following the common protocol in the community [1,4,23,43], we perform the zero-shot Chinese character recognition benchmarks on the HWDB [24] and the CTW [50] dataset following [4,23,43]. The model is trained for 50k iterations due to the small size of the training set. As shown in Table 2, our method shows a significant performance advantage over existing methods. Qualitative samples in Fig. 8 show some robustness over style diversity, slight blur, and other confounding factors. This also suggests that some degenerates like blur or low-contrast do not necessarily yield permanent information

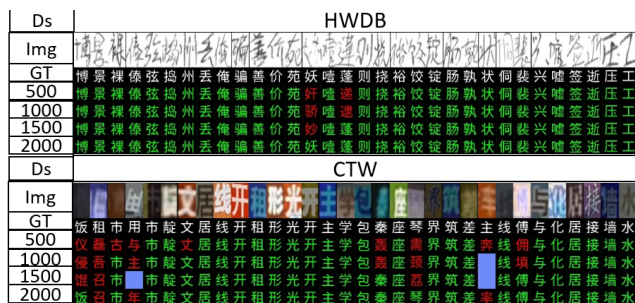


Figure 8. Sample results on the zero-shot Chinese **Character** recognition benchmarks. Numbers on the left indicates the number of different classes used for training. Green indicates correct recognition results, Red indicates wrong ones, and purple block indicates rejections. Note white does not indicate seen characters, **all** test characters are novel.

loss and could be inverted with sufficient well-distributed training data. We owe part of the robustness difference between open-set word recognition and this challenge to the potential language-specific “image style” bias, caused by factors including different cameras, picture-taking habits in different corresponding region.

These experiments demonstrate reasonable generalization capability compared to the SOTA zero-shot character recognition methods. This also justifies the choice of the data-driven latent representation against model-driven representations like the radical sequences [4,6]. Our method does not require structural knowledge of characters, which enables potential use to recognize Oracles and other ligatures where such knowledge is unknown or not applicable.

Close-Set Benchmarks Finally, we perform experiments on the conventional close-set benchmarks, where the method is compared to SOTA text recognition methods performance-wise and speed-wise. We report both dictionary-free performance (Table 3) and dictionary-based

Table 3. Performance on conventional close-set benchmarks. * indicates character-level annotation and + for multi-batch evaluation.

Methods	Venue	Training Set	RNN	FPS	IIIT5K	SVT	IC03	IC13	CUTE
Comb.Best [2]	ICCV'19	MJ+ST	Y	36.23	87.9	87.5	94.4	92.3	71.8
SAR [20]	AAAI'19	MJ+ST	Y	-	91.5	84.5	-	-	83.3
ESIR [51]	CVPR'19	MJ+ST	Y	-	93.3	90.2	-	-	83.3
SCATTER [22]	CVPR'20	MJ+ST+Extra	Y	-	93.7	92.7	96.3	93.9	87.5
SEED [29]	CVPR'20	MJ+ST	Y	-	93.8	89.6	-	92.8	83.6
DAN [44]	AAAI'20	MJ+ST	Y	-	94.3	89.2	95.0	93.9	84.4
Rosetta [3] [2]	KDD'18	MJ+ST	N	212.76	84.3	84.7	92.9	89.0	69.2
CA-FCN* [21]	AAAI'19	ST	N	45	92.0	82.1	-	91.4	78.1
TextScanner* [40]	AAAI'20	MJ+ST+Extra	N	-	93.9	90.1	-	92.9	83.3
Ours-Large	-	MJ+ST	N	66.91/255 ⁺	91.90	85.93	92.38	92.21	83.68

Table 4. Experiments on lexicon-based close-set benchmarks. ^c indicates close-set methods and * indicates datasets other than MJ and ST are used.

Method	Venue	IIIT5k (small/middle)	IC03 (full)	SVT (50)
AON ^c [9]	CVPR'18	99.6/98.1	96.7	96
ESIR ^c [51]	CVPR'19	99.6/98.8	-	97.4
CA-FCN ^{c*} [21]	AAAI'19	99.8/98.9	-	98.5
Zhang <i>et al.</i> [52]	ECCV'20	96.2/92.8	93.3	92.4
OSOCR-L [23]	-	99.5/98.6	96.7	96.7
Ours-L	-	99.8/99.0	96.9	97.9

performance [52]. More specifically, the model is trained on MJ [17] and ST [14] following the mainstream technique of SOTA methods. For evaluation, IIIT5k [27], SVT [42], ICDAR 2003 [25], ICDAR 2013 [18], and CUTE [32] are used. Our model is trained for 800k iterations due to the significantly larger training set.

We first compare our method to other open-set text recognition methods that report their performances on lexicon-based benchmarks in Table 4, together with some popular close-set recognition methods. Results show our method retains reasonable close-set performance compared to other open-set methods. Our method also reaches close performance against SOTA close-set methods on this benchmark. Second, comparisons using the dictionary-free protocol are shown in Table 3, despite the performances being slightly lower than the heavy SOTA close-set recognition methods to trade for faster speed, our method shows competitive performance against lightweight text recognition methods. Following community convention [2, 21], running speed is adopted to measure the cost of the method. Our method can reach 67 FPS single batched and 255 FPS multi-batched on a laptop with an RTX 2070 Mobile GPU

(7 TFlops), while only using 2.5 GiB Vram. This justifies our model as a competitive light-weight method for conventional tasks.

5. Limitations

Despite showing reasonable performances on all tested scenarios, our method still has some limitations. Framework-wise, we made a few strong assumptions. First, we assume the visual feature extractor can be generalized to a new language. Despite showing better intra-language transferring capability than radical-based methods, it is a little bit too strong to assume robust inter-language transferring capability. These limitations could be causing the performance gap between Kanas and Unique kanjis. Implementation-wise, our method uses a small input (32 * 128 patches) and lacks effective rectification modules [26, 35]. This leads to a very small effective text area, hence limiting the performance of skewed and curvy samples. We will discuss how to address these limitations in our next work.

6. Conclusion

In this paper, we propose a Character-Context Decoupling Framework for open-set text recognition, which is theoretically sound and experimentally feasible. Specifically, the ablative studies and comparative experiments verify that our implementation is an effective open-set text recognition method and a production-ready lightweight text recognition method under close-set scenarios.

7. Acknowledgement

The research is partly supported by the National Key Research and Development Program of China (2020AAA09701), The National Science Fund for Distinguished Young Scholars (62125601), and the National Natural Science Foundation of China (62006018, 62076024).

References

- [1] Xiang Ao, Xu-Yao Zhang, Hong-Ming Yang, Fei Yin, and Cheng-Lin Liu. Cross-modal prototype learning for zero-shot handwriting recognition. In *ICDAR*, pages 589–594, 2019. [2](#), [7](#)
- [2] Jeonghun Baek, Geewook Kim, Junyeop Lee, Sungrae Park, Dongyoon Han, Sangdoon Yun, Seong Joon Oh, and Hwal-suk Lee. What is wrong with scene text recognition model comparisons? dataset and model analysis. In *ICCV*, pages 4714–4722, 2019. [8](#)
- [3] Fedor Borisjuk, Albert Gordo, and Viswanath Sivakumar. Rosetta: Large scale system for text detection and recognition in images. In *KDD*, pages 71–79, 2018. [2](#), [8](#)
- [4] Zhong Cao, Jiang Lu, Sen Cui, and Changshui Zhang. Zero-shot handwritten Chinese character recognition with hierarchical decomposition embedding. *Pattern Recognition*, 107:107488, 2020. [2](#), [7](#), [13](#)
- [5] Woong-Gi Chang, Tackgeun You, Seonguk Seo, Suha Kwak, and Bohyung Han. Domain-specific batch normalization for unsupervised domain adaptation. In *CVPR*, pages 7354–7362, 2019. [3](#), [4](#), [12](#)
- [6] Jingye Chen, Bin Li, and Xiangyang Xue. Zero-shot Chinese character recognition with stroke-level decomposition. In *IJCAI*, pages 615–621, 2021. [2](#), [7](#)
- [7] Xiaoxue Chen, Lianwen Jin, Yuanzhi Zhu, Canjie Luo, and Tianwei Wang. Text recognition in the wild: A survey. *ACM Comput. Surv.*, 54(2):42:1–42:35, 2021. [1](#)
- [8] Ye Chen, Hongchun Shu, Wenjiao Xu, Zhengyu Yang, Zhihu Hong, and Mingshuai Dong. Transformer text recognition with deep learning algorithm. *Comput. Commun.*, 178:153–160, 2021. [14](#)
- [9] Zhanzhan Cheng, Yangliu Xu, Fan Bai, Yi Niu, Shiliang Pu, and Shuigeng Zhou. AON: Towards arbitrarily-oriented text recognition. In *CVPR*, pages 5571–5579, 2018. [3](#), [8](#)
- [10] Chee Kheng Chng, Errui Ding, Jingtuo Liu, Dimosthenis Karatzas, Chee Seng Chan, Lianwen Jin, Yuliang Liu, Yipeng Sun, Chun Chet Ng, Canjie Luo, Zihan Ni, Chuan-Ming Fang, Shuaitao Zhang, and Junyu Han. ICDAR2019 robust reading challenge on arbitrary-shaped text (RRC-ArT). In *ICDAR*, pages 1571–1576, 2019. [13](#)
- [11] Shancheng Fang, Hongtao Xie, Yuxin Wang, Zhendong Mao, and Yongdong Zhang. Read like humans: Autonomous, bidirectional and iterative language modeling for scene text recognition. In *CVPR*, pages 7098–7107, 2021. [2](#), [4](#), [14](#)
- [12] Xinjie Feng, Hongxun Yao, Yuankai Qi, Jun Zhang, and Shengping Zhang. Scene text recognition via transformer. *CoRR*, abs/2003.08077, 2020. [14](#)
- [13] Chuanxing Geng, Sheng-Jun Huang, and Songcan Chen. Recent advances in open set recognition: A survey. *IEEE Trans. Pattern Anal. Mach. Intell.*, 43(10):3614–3631, 2021. [2](#)
- [14] Ankush Gupta, Andrea Vedaldi, and Andrew Zisserman. Synthetic data for text localisation in natural images. In *CVPR*, pages 2315–2324, 2016. [8](#), [13](#)
- [15] Jie-Bo Hou, Xiaobin Zhu, Chang Liu, Kekai Sheng, Long-Huang Wu, Hongfa Wang, and Xu-Cheng Yin. HAM: Hidden anchor mechanism for scene text detection. *IEEE Trans. Image Process.*, 29:7904–7916, 2020. [4](#), [11](#)
- [16] Yuhao Huang, Lianwen Jin, and Dezhi Peng. Zero-shot Chinese text recognition via matching class embedding. In *ICDAR*, volume 12823, pages 127–141, 2021. [1](#), [2](#)
- [17] Max Jaderberg, Karen Simonyan, Andrea Vedaldi, and Andrew Zisserman. Synthetic data and artificial neural networks for natural scene text recognition. *CoRR*, abs/1406.2227, 2014. [8](#), [13](#)
- [18] Dimosthenis Karatzas, Faisal Shafait, Seiichi Uchida, Masakazu Iwamura, Lluís Gomez i Bigorda, Sergi Robles Mestre, Joan Mas, David Fernández Mota, Jon Almazán, and Luíís-Pere de las Heras. ICDAR 2013 robust reading competition. In *ICDAR*, pages 1484–1493, 2013. [8](#)
- [19] Diederik P. Kingma and Max Welling. Auto-encoding variational bayes. In Yoshua Bengio and Yann LeCun, editors, *ICLR*, 2014. [5](#)
- [20] Hui Li, Peng Wang, Chunhua Shen, and Guyu Zhang. Show, attend and read: A simple and strong baseline for irregular text recognition. In *AAAI*, pages 8610–8617, 2019. [2](#), [8](#)
- [21] Minghui Liao, Jian Zhang, Zhaoyi Wan, Fengming Xie, Jiajun Liang, Pengyuan Lyu, Cong Yao, and Xiang Bai. Scene text recognition from two-dimensional perspective. In *AAAI*, pages 8714–8721, 2019. [3](#), [8](#)
- [22] Ron Litman, Oron Anshel, Shahar Tsiper, Roe Litman, Shai Mazor, and R. Manmatha. SCATTER: Selective context attentional scene text recognizer. In *CVPR*, pages 11959–11969, 2020. [8](#)
- [23] Chang Liu, Chun Yang, Hai-Bo Qin, Xiaobin Zhu, Jie-Bo Hou, and Xu-Cheng Yin. Towards open-set text recognition via label-to-prototype learning. *CoRR*, abs/2203.05179v1, 2021. [1](#), [2](#), [5](#), [6](#), [7](#), [8](#), [12](#), [13](#)
- [24] Cheng-Lin Liu, Fei Yin, Da-Han Wang, and Qiu-Feng Wang. CASIA online and offline Chinese handwriting databases. In *ICDAR*, pages 37–41, 2011. [7](#)
- [25] Simon M. Lucas, Alex Panaretos, Luis Sosa, Anthony Tang, Shirley Wong, Robert Young, Kazuki Ashida, Hiroki Nagai, Masayuki Okamoto, Hiroaki Yamamoto, Hidetoshi Miyao, JunMin Zhu, WuWen Ou, Christian Wolf, Jean-Michel Jolion, Leon Todoran, Marcel Worring, and Xiaofan Lin. ICDAR 2003 robust reading competitions: entries, results, and future directions. *Int. J. Document Anal. Recognit.*, 7(2-3):105–122, 2005. [8](#)
- [26] Canjie Luo, Lianwen Jin, and Zenghui Sun. MORAN: A multi-object rectified attention network for scene text recognition. *Pattern Recognition*, 90:109–118, 2019. [8](#)
- [27] A. Mishra, K. Alahari, and C. V. Jawahar. Scene text recognition using higher order language priors. In *BMVC*, pages 127.1–127.11, 2012. [8](#)
- [28] Nibal Nayef, Yash Patel, Michal Busta, Pinaki Nath Chowdhury, Dimosthenis Karatzas, Wafa Khelif, Jiri Matas, Uma-pada Pal, Jean-Christophe Burie, and Cheng-Lin Liu. ICDAR2019 robust reading challenge on multi-lingual scene text detection and recognition (RRC-MLT-2019). In *ICDAR*, pages 1582–1587, 2019. [13](#)
- [29] Zhi Qiao, Yu Zhou, Dongbao Yang, Yucan Zhou, and Weiping Wang. SEED: Semantics enhanced encoder-decoder

- framework for scene text recognition. In *CVPR*, pages 13525–13534, 2020. 8
- [30] Joseph Redmon and Ali Farhadi. YOLO9000: Better, faster, stronger. In *CVPR*, pages 6517–6525, 2017. 5
- [31] Shaoqing Ren, Kaiming He, Ross B. Girshick, and Jian Sun. Faster R-CNN: Towards real-time object detection with region proposal networks. *IEEE Trans. Pattern Anal. Mach. Intell.*, 39(6):1137–1149, 2017. 5
- [32] Anhar Risnumawan, Palaiahnakote Shivakumara, Chee Seng Chan, and Chew Lim Tan. A robust arbitrary text detection system for natural scene images. *Expert Syst. Appl.*, 41(18):8027–8048, 2014. 8
- [33] Walter J. Scheirer, Anderson de Rezende Rocha, Archana Sapkota, and Terrance E. Boult. Toward open set recognition. *IEEE Trans. Pattern Anal. Mach. Intell.*, 35(7):1757–1772, 2013. 1, 2
- [34] Baoguang Shi, Xiang Bai, and Cong Yao. An end-to-end trainable neural network for image-based sequence recognition and its application to scene text recognition. *IEEE Trans. Pattern Anal. Mach. Intell.*, 39(11):2298–2304, 2017. 2, 3
- [35] Baoguang Shi, Mingkun Yang, Xinggang Wang, Pengyuan Lyu, Cong Yao, and Xiang Bai. ASTER: an attentional scene text recognizer with flexible rectification. *IEEE Trans. Pattern Anal. Mach. Intell.*, 41(9):2035–2048, 2019. 3, 8
- [36] Baoguang Shi, Cong Yao, Minghui Liao, Mingkun Yang, Pei Xu, Linyan Cui, Serge J. Belongie, Shijian Lu, and Xiang Bai. ICDAR2017 competition on reading Chinese text in the wild (RCTW-17). In *ICDAR*, pages 1429–1434, 2017. 13
- [37] Karen Simonyan, Andrea Vedaldi, and Andrew Zisserman. Deep inside convolutional networks: Visualising image classification models and saliency maps. In *ICLR*, 2014. 1
- [38] Yipeng Sun, Dimosthenis Karatzas, Chee Seng Chan, Lianwen Jin, Zihan Ni, Chee Kheng Chng, Yuliang Liu, Canjie Luo, Chun Chet Ng, Junyu Han, Errui Ding, and Jingtuo Liu. ICDAR 2019 competition on large-scale street view text with partial labeling (RRC-LSVT). In *ICDAR*, pages 1557–1562, 2019. 13
- [39] Ashish Vaswani, Noam Shazeer, Niki Parmar, Jakob Uszkoreit, Llion Jones, Aidan N Gomez, Łukasz Kaiser, and Illia Polosukhin. Attention is all you need. In *NeurIPS*, pages 5998–6008, 2017. 5
- [40] Zhaoyi Wan, Minghang He, Haoran Chen, Xiang Bai, and Cong Yao. Textscanner: Reading characters in order for robust scene text recognition. In *AAAI*, pages 12120–12127, 2020. 3, 8
- [41] Zhaoyi Wan, Jielei Zhang, Liang Zhang, Jiebo Luo, and Cong Yao. On vocabulary reliance in scene text recognition. In *CVPR*, pages 11422–11431, 2020. 1, 2
- [42] Kai Wang, Boris Babenko, and Serge J. Belongie. End-to-end scene text recognition. In *ICCV*, pages 1457–1464, 2011. 8
- [43] Tianwei Wang, Zecheng Xie, Zhe Li, Lianwen Jin, and Xian-gle Chen. Radical aggregation network for few-shot offline handwritten Chinese character recognition. *Pattern Recognition Letters*, 125:821–827, 2019. 2, 7
- [44] Tianwei Wang, Yuanzhi Zhu, Lianwen Jin, Canjie Luo, Xiaoxue Chen, Yaqiang Wu, Qianying Wang, and Mingxiang Cai. Decoupled attention network for text recognition. In *AAAI*, pages 12216–12224, 2020. 2, 3, 8, 12, 13, 14
- [45] Wenchao Wang, Jianshu Zhang, Jun Du, Zi-Rui Wang, and Yixing Zhu. Denseran for offline handwritten Chinese character recognition. In *ICFHR*, pages 104–109, 2018. 2
- [46] Wenchao Wang, Jianshu Zhang, Jun Du, Zi-Rui Wang, and Yixing Zhu. Denseran for offline handwritten Chinese character recognition. In *ICFHR*, pages 104–109, 2018. 7
- [47] M.P. Wellman and M. Henrion. Explaining ‘explaining away’. *IEEE Trans. Pattern Anal. Mach. Intell.*, 15(3):287–292, 1993. 2, 4
- [48] Zecheng Xie, Yaoxiong Huang, Yuanzhi Zhu, Lianwen Jin, Yuliang Liu, and Lele Xie. Aggregation cross-entropy for sequence recognition. In *CVPR*, pages 6538–6547, 2019. 2
- [49] Deli Yu, Xuan Li, Chengquan Zhang, Tao Liu, Junyu Han, Jingtuo Liu, and Errui Ding. Towards accurate scene text recognition with semantic reasoning networks. In *CVPR*, pages 12110–12119, 2020. 2, 4, 14
- [50] Tai-Ling Yuan, Zhe Zhu, Kun Xu, Cheng-Jun Li, Tai-Jiang Mu, and Shi-Min Hu. A large Chinese text dataset in the wild. *J. Comput. Sci. Technol.*, 34(3):509–521, 2019. 7, 13
- [51] Fangneng Zhan and Shijian Lu. ESIR: end-to-end scene text recognition via iterative image rectification. In *CVPR*, pages 2059–2068, 2019. 8
- [52] Chuhan Zhang, Ankush Gupta, and Andrew Zisserman. Adaptive text recognition through visual matching. In *ECCV*, pages 51–67, 2020. 1, 2, 8
- [53] Chang-Bin Zhang, Peng-Tao Jiang, Qibin Hou, Yunchao Wei, Qi Han, Zhen Li, and Ming-Ming Cheng. Delving deep into label smoothing. *IEEE Trans. Image Process.*, 30:5984–5996, 2021. 6
- [54] Xu-Yao Zhang, Cheng-Lin Liu, and Ching Y. Suen. Towards robust pattern recognition: A review. *Proceedings of IEEE*, 108(6):894–922, 2020. 1
- [55] Yiwei Zhu, Shilin Wang, Zheng Huang, and Kai Chen. Text recognition in images based on transformer with hierarchical attention. In *ICIP*, pages 1945–1949, 2019. 14

A. Proof of Theorem 1

Assumption 1 (A1) We assume the linguistic information functions as a common-cause of the input visual information and the prediction outputs at all timestamps (See Fig. 3). We model the sample image as a “rendered” result of the label \mathbf{y} . Also, we assume the label (words) is generated according to linguistic information c , making the label \mathbf{y} a causal result of c . Hence, linguistic context c and the character-level visual information $x_{[t]}$ are the only two direct factors affecting the probability of $y_{[t]}$ at timestamp t ,

$$\begin{aligned} & P(y_{[t]}|x_{[t]}, \mathbf{x}, y_{[t-1]} \dots y_{[0]}, l, c) \\ \stackrel{(a)}{=} & P(y_{[t]}|x_{[t]}, \mathbf{x}, Pre_{[t]}, l, c) \\ = & P(y_{[t]}|x_{[t]}, c), \end{aligned} \quad (16)$$

where we denote prefix of $y_{[t]}$ as $Pre_{[t]}$ in (a).

Proof.

$$\begin{aligned} & P(\mathbf{y}|\mathbf{x}, l) \\ = & \prod_{t=1}^l P(y_{[t]}|\mathbf{x}, l, y_{[t-1]} \dots y_{[0]}) \\ = & \prod_{t=1}^l \int_{c \in C_{[t]}} P(y_{[t]}|\mathbf{x}, Pre_{[t]}, l, c) P(c|\mathbf{x}, l) \\ \stackrel{(a)}{=} & \prod_{t=1}^l \int_{c \in C_{[t]}} P(y_{[t]}|x_{[t]}, c) P(c|\mathbf{x}, l). \end{aligned} \quad (17)$$

□

Here, (a) is derived by applying Eq. 16 of Assumption A1. The integral term can be interpreted as an ensemble of “anchored prediction” $P(y_{[t]}|x_{[t]}, c)$ over all possible contexts c , which is similar to the hidden anchor mechanism [15]. Hence, we call this theorem the anchor property of context.

B. Proof of Theorem 2

Assumption 2 (A2) The shape (character visual information) of a character and its context (linguistic information) are independent given the character $y_{[t]}$, i.e.,

$$\begin{aligned} & P(x_{[t]}|y_{[t]}, c) = P(x_{[t]}|y_{[t]}) \\ \iff & P(x_{[t]}, c|y_{[t]}) = P(x_{[t]}|y_{[t]})P(c|y_{[t]}) \end{aligned} \quad (18)$$

Theorem 2: The Separable Property of Linguistic Information and Character Visual Information

Given assumption A2 holds, the effect of character visual information over label $P(y_{[t]}|x_{[t]})$ and the effect

of $P(y_{[t]}|c)$ can be separated from contextual prediction $P(y_{[t]}|x_{[t]}, c)$:

$$\begin{aligned} & P(y_{[t]}|x_{[t]}, c) \\ \propto & \frac{P(y_{[t]}|x_{[t]})P(y_{[t]}|c)}{P(y_{[t]})} \\ := & Pr(y_{[t]}, x_{[t]}, c) \end{aligned} \quad (19)$$

Proof.

$$\begin{aligned} & P(y_{[t]}|x_{[t]}, c) \\ = & \frac{P(x_{[t]}, y_{[t]}, c)}{P(x_{[t]}, c)} \\ = & \frac{P(x_{[t]}, c|y_{[t]})P(y_{[t]})}{P(x_{[t]}, c)} \\ \stackrel{(a)}{=} & \frac{P(x_{[t]}|y_{[t]})P(c|y_{[t]})P(y_{[t]})}{P(x_{[t]}, c)} \\ = & \frac{P(y_{[t]})}{P(x_{[t]}, c)} P(x_{[t]}|y_{[t]}) P(c|y_{[t]}) \\ = & \frac{P(y_{[t]})}{P(x_{[t]}, c)} \frac{P(y_{[t]}|x_{[t]})P(x_{[t]})}{P(y_{[t]})} \frac{P(y_{[t]}|c)P(c)}{P(y_{[t]})} \\ = & P(y_{[t]}|c)P(y_{[t]}|x_{[t]}) \frac{P(x_{[t]})P(c)}{P(x_{[t]}, c)P(y_{[t]})} \\ = & \frac{P(y_{[t]}|x_{[t]})P(y_{[t]}|c)}{P(y_{[t]})} \frac{P(x_{[t]})}{P(x_{[t]}|c)} \\ = & Pr(y_{[t]}, x_{[t]}, c) \frac{P(x_{[t]})}{P(x_{[t]}|c)} \\ = & Pr(y_{[t]}, x_{[t]}, c) \frac{P(x_{[t]})}{\sum_{y'_{[t]} \in \mathcal{Y}} P(x_{[t]}|y'_{[t]}, c) P(y'_{[t]}|c)} \\ \stackrel{(b)}{=} & Pr(y_{[t]}, x_{[t]}, c) \frac{P(x_{[t]})}{\sum_{y'_{[t]} \in \mathcal{Y}} P(x_{[t]}|y'_{[t]}) P(y'_{[t]}|c)} \\ \stackrel{(c)}{=} & \frac{Pr(y_{[t]}, x_{[t]}, c)}{\sum_{y'_{[t]} \in \mathcal{Y}} Pr(y'_{[t]}, x_{[t]}, c)} \\ \stackrel{(d)}{\propto} & Pr(y_{[t]}, x_{[t]}, c). \end{aligned} \quad (20)$$

□

Here, \mathcal{Y} is the character set. Step (a) and (b) is derived using Eq. 18 in assumption A2. Step (c) is derived by applying Bayesian rule over $P(x_{[t]}|y'_{[t]})$ and canceling $x_{[t]}$. Although $\sum_{y'_{[t]} \in \mathcal{Y}} Pr(y'_{[t]}, x_{[t]}, c)$ is not a constant number and may vary with timestamp t , but it is the same for all label $y'_{[t]}$ at a certain timestamp t , hence step (d) holds, despite the constant factor can change.

C. Proof of Theorem 3

Combining Theorem 1 and Theorem 2, we have the Decoupled Context Anchor mechanism,

$$P(\mathbf{y}|\mathbf{x}, l) = \prod_{t=1}^l P(y_{[t]}|x_{[t]}) \prod_{t=1}^l \int^{c \in C_{[t]}} P(y_{[t]}|c)P(c|\mathbf{x}, l). \quad (21)$$

Proof.

$$\begin{aligned} P(\mathbf{y}|\mathbf{x}, l) &= \prod_{t=1}^l \int^{c \in C_{[t]}} P(y_{[t]}|x_{[t]}, c)P(c|\mathbf{x}, l) \\ &\propto \prod_{t=1}^l \int^{c \in C_{[t]}} \frac{P(y_{[t]}|x_{[t]})P(y_{[t]}|c)}{P(y_{[t]})} P(c|\mathbf{x}, l) \\ &= \alpha \prod_{t=1}^l \frac{P(y_{[t]}|x_{[t]})}{P(y_{[t]})} \prod_{t=1}^l \int^{c \in C_{[t]}} P(y_{[t]}|c)P(c|\mathbf{x}, l), \\ &= \beta(\mathbf{y}) \prod_{t=1}^l P(y_{[t]}|x_{[t]}) \prod_{t=1}^l \int^{c \in C_{[t]}} P(y_{[t]}|c)P(c|\mathbf{x}, l), \\ &:= \prod_{t=1}^l P(y_{[t]}|x_{[t]}) \prod_{t=1}^l \int^{c \in C_{[t]}} P(y_{[t]}|c)P(c|\mathbf{x}, l), \end{aligned} \quad (22)$$

□

The visual prediction can be taken out of the integral as it is not affected by the linguistic information, i.e., c . Here,

$$\beta(\mathbf{y}) = \frac{\alpha}{\prod_1^l P(y_t)}, \quad (23)$$

and it is a character frequency term related to the word. During training, $\beta(\mathbf{y}^*)$ only associates with the label, hence would be constant for a certain label and won't produce gradient. During the evaluation, as the dictionary and character frequency are unknown, character frequency would be assumed as uniform, resulting in $\beta(\mathbf{y})$ being a constant number $\frac{\alpha}{|C_{eval}|^l}$ for all words with length l . Hence, despite varying from word to word, treating it as a constant does not affect either training or evaluation. As a result, β is omitted for writing convenience.

D. An Engineering Perspective of OpenCCD

While the main paper puts more stress on the theoretical part of the framework, we present an engineering perspective of the OpenCCD framework which focuses on how things are implemented over what each module does.

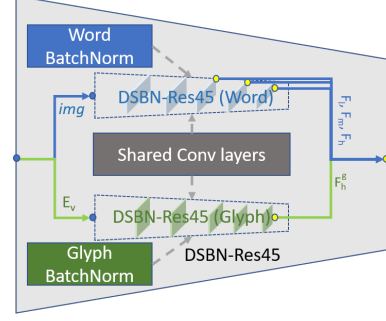


Figure 9. The DSBN-Res45 backbone.

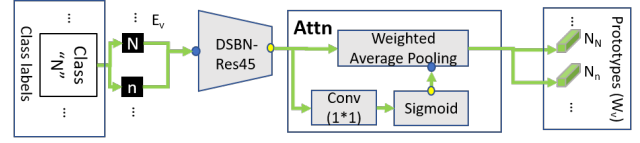


Figure 10. The prototype generation process.

D.1. DSBN-Res45

In this work, the DSBN-Res45 (Fig. 9) is used to encode word images and glyphs into corresponding visual features. The DSBN-Res45 backbone is a modified version of the 45-layer ResNet used in [44]. Here, we replaced all its batch norm layers with re-implemented DSBN [5] layers. This adaption is made to alleviate the impact of the bias between the word image domain and the glyph domain. Specifically, the network uses the same set of convolution kernels for both word-level images and glyph images, while using the domain-specific batch statistics for normalization of each specific domain. The layout of the regular model is similar to the original DAN implementation [44], and the large model simply adds more latent channels to the backbone, and further details like specific network layout can be found in the released code. This module is a part of the base model and is used in **all** models in ablative studies.

D.2. Prototype Generation

The prototypes generation process is shown in Fig. 10 for each class, the framework first extracts corresponding visual features of each glyph with the backbone. Then spatial attention is applied to reduce the feature map to a single feature via the Attn Module. Specifically, the module first estimates the foreground/background attention mask with a convolution layer, then reduces and normalizes the feature map into corresponding prototypes. Same to [23], a label may possess more than one prototype as each character can have different ‘‘cases’’, e.g., ‘N’ and ‘n’. The prototypes are normalized to alleviate character-frequency related bias. This module is also a part of the base model and is used in **all** models in ablative studies.

Table 5. Important notations in the paper with first occurrence and their brief explanations.

Notation	Occurrence	Explanation
N	-	Number of glyphs ('N' and 'n' has the same label)
M	-	Number of characters (labels)
E	Fig.2	The collection of the glyph (E_v) and semantic embedding (E_c)
E_c	Fig.2	The collection of the glyph (E_v) for characters. Each character can have several glyphs according to how many cases it has.
E_v	Fig.2	The semantic embedding (E_c) for characters. Each character only has one embedding in our framework.
W_v	Fig.2	Prototypes generated from E_v . $W_v : R^{N \times D}$, $N = E_v $ and $D = 512$
$\hat{\mathbf{y}}$	Eq. 1	Predicted word label, consisted of a ordered sequence of predicted character labels $\hat{y}_{[t]}$.
\mathbf{y}	Eq. 1	Any word label, consisted of a ordered sequence of character labels $y_{[t]}$.
$\hat{y}_{[t]}$	Eq. 1	t^{th} predicted character.
θ	Eq. 1	The trainable parameters of the framework.
\mathbf{x}	Eq. 1	character visual information of all characters in a word
l	Eq. 2	Length of a sequence.
$x_{[t]}$	Eq. 3	character visual information of the t^{th} character in the word
c	Eq. 3	Linguistic information.
\mathbf{y}^*	Eq. 4	Ground truth word label, consisted of a ordered sequence of ground truth character labels $y_{[t]}^*$.
l^*	Eq. 4	Length of the ground truth word.
$C_{[t]}$	Eq. 4	All possible Linguistic information.
L_{len}	Eq. 4	Minus likelihood of the correct length being predicted: $-\log P(l^* \mathbf{x})$
L_{vis}	Eq. 4	Minus likelihood of the correct word being predicted according to character visual information: $-\sum_{t=1}^{l^*} (\log P(y_{[t]}^* x_{[t]}))$
L_{vis}	Eq. 4	Minus likelihood of the correct word being predicted according to linguistic information: $-\sum_{t=1}^l \log(\int^{c \in C_{[t]}} P(y_{[t]}^* c)P(c \mathbf{x}, l^*))$
$y_{[t]}$	Eq. 5	Any t^{th} character, applies to any possible character in the character set (means it applies to predicted and ground truth as well.)
ψ	Ch3.3.3	Function indexes all corresponding prototypes of the input label $y_{[t]}$.
w_v	Ch3.3.3	A row in W_v .
\hat{c}	Ch3.3.4	Context predicted via transformer. $\hat{c} \in R^{l \times D}$
$\mathbf{Y}_{[t]}$	Ch3.3.4	The probability distribution at time stamp t : $P(\mathbf{Y}_{[t]} x_{[t]}) : (P(y_{[t]}^0 x_{[t]}), \dots, P(y_{[t]}^M x_{[t]}))$
Y	Ch3.3.4	The probability distribution at all time stamps: $Y \in (0, 1)^{l \times M} : (P(\mathbf{Y}_{[0]} x_{[0]}), \dots, P(\mathbf{Y}_{[l]} x_{[l]}))$

D.3. Data, Training, and Evaluation

The training and evaluation and models for most experiments (all except dictionary-based close-set experiments) are now released to Kaggle⁴. For the open-set task, the training dataset is built by aggregating the following datasets: RCTW [36], Chinese and Latin subset of the MLT-2019 dataset [28], LSVT [38], ART [10], and CTW [50]. The training character set contains 3755 Tire-1 Simplified Chinese characters, 52 Latin characters, and 10 digits. Vertical Samples and samples containing characters outside of the training character set are removed from the training set

(samples with Tradition Chinese Characters are removed as well). The evaluation dataset contains 4009 horizontal images from the Japanese subset of the MLT-2019 dataset and the testing character set includes 1460 characters appearing in the evaluation set, making a total of 1461 different classes adding the “unknown” class. For the close-set model, we use exactly the same datasets as DAN [44], which adopts the most used MJ [17]-ST [14] combo as the training set. For the zero-shot Character recognition tasks, we reuse the split from OSOCR [23], which follows HCCR’s protocol [4]. Note that like HCCR [4], few methods made the exact split of seen and novel characters public.

⁴<https://www.kaggle.com/vsdf2898kaggle/osocrtraining>

During training, a label sampler is used to sample a sub-

set of characters during each iteration like OSOCR. For word-level tasks, the model processes data is similar to DAN [44]. Specifically, the model takes 32*128 RGB clips, where the images are resized keeping aspect ratio and center-padded into 32*128 with zeros for both training and testing. The common dictionary-free protocols are used for all word-level evaluations. For character recognition tasks, the model treats character images like word images, despite the clip size being set as 32*64 to speed up. For all three tasks, we use NotoFont as the glyph provider, where each character is rendered and centered to 32*32 binary patches. The training processes are mostly the same with DAN [44] except for adding a prototype generation process.

For evaluation, the most popular evaluation protocol, the Line Accuracy is used to measure word recognition performance following the community. The Character Accuracy (1-NED) is also used as compensation for open-set word recognition tasks to give an intuitive insight on the recognition quality per character. For the zero-shot Chinese Character recognition task, Character Accuracy and Line Accuracy is the same number, simply called Accuracy by the community.

E. Extra Details

E.1. Notations

We made a notation table (Table 5) to include all used notations in this paper. In most cases, hat ($\hat{\cdot}$) indicate the max probable prediction, and asterisk (\cdot^*) indicates the ground truth. **Bold** notations indicate vectors and capital alphabets indicate matrices, sets, or distributions.

E.2. About Related Work

Despite the proposed Decoupled Context Anchor mechanism (DCA) uses a transformer to model contextual information, this work is not directly related to the transformer-based methods [8, 12, 55]. Structure-wise, the transformer in our method is a BERT-style transformer encoder, also used in [11, 49], while [8, 12, 55] uses GPT-style transformer decoders. Purpose-wise, the transformer in this work is used as a regularization term (which is the direct reason we backpropagate to the feature encoder). Instead, [11, 49] use the transformer as a post-process module by cutting the gradient flow (Note [49] did not clarify this in their paper, but you can see it from their officially released code). Conventional transformer-based methods directly decode the CNN features into prediction sequences. Therefore, the DCA module is different in terms of structure and motivation.